

The X-Ray Examination of Selenium Crystals

By

Kenzo Tanaka

(Received January 15, 1934)

Abstract

Several forms of metallic selenium crystals obtained by the condensation of selenium vapour were examined by means of X-rays. The crystal of metallic selenium grows most prominently in its trigonal axis. This growth process of the selenium crystal is interpreted from the standpoint of the theory of the growth of homopolar crystals.

The degree of perfection and the size of the grain of selenium crystals were estimated from the fine structure of the spectral lines obtained with convergent X-rays. The intensity distribution along the spectral line was interpreted from the intensity distribution of the primary X-rays at various starting points on the surface of the anticathode.

The transition point from the vitreous to the metallic form was determined both by X-ray examination and by measurement of the net densities.

Introduction

Selenium has three distinct allotropic forms. These are liquid selenium, including vitreous and amorphous selenium, crystalline red selenium and crystalline metallic selenium. Of the last modification Brown¹ observed three distinct types of crystals produced by the condensation of the vapour given off by molten selenium placed in a glass tube and heated to about 270° either in a high vacuum or in the air at atmospheric pressure. The first type of these crystals was rhombohedral or hexagonal in shape and the second type grew in clusters of needles in which well-developed crystals had six surfaces. The third type consisted of thin flexible sheets. In addition to these three types of crystals he described the occurrence of lamellar crystals

1 F. C. Brown: Phys. Rev. 4, 85 (1914)

„ 5, 236 (1915)

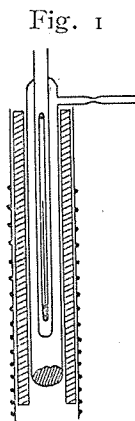
belonging to the monoclinic system. Kahler¹ compared the selenium crystals obtained by condensation of the vapour and those obtained by cathodic sputtering, with regard to their structure.

Later, Bradley² obtained by the condensation of the vapour only one type of metallic selenium crystal, which resembled in outer shape the lamellar crystals described by Brown. He also determined the crystal structure of metallic selenium by the X-ray powder method.

The present investigation was made to examine these several types of selenium crystals with X-rays and to find how the micro-crystals of selenium are arranged in these crystals.

Experimental Method

Vitreous selenium sticks (Merk) were placed between two glass cylindrical vessels of about 3 cms. in outside diameter and 35 cms. in length as shown in Fig. 1. To obtain a uniform temperature gradient all along the vessel, it was covered by a metal tube which was heated by an electric furnace. The heating current of the furnace was supplied from batteries. The temperatures along the inner glass tube were indicated by a mercury thermometer inserted in it. Evacuation was still carefully continued for some hours after the temperature had become steady and the vessel was afterwards sealed at a side tube. The condensation of the vapour went on for four or five days. The temperature at the bottom of the inner glass tube was maintained at 280° and the temperature of the molten selenium was about 5° higher than that. In some cases, the vapour was allowed to condense in the air at atmospheric pressure.



The crystals thus deposited on the outer wall of the inner glass tube were examined by X-rays from a metallic Shearer tube with a Cu anticathode. For the determination of the orientation of the crystal and of the arrangement of the micro-crystals from the X-ray photographs, the crystallographic globe³ was used.

1 H. Kahler: *Phys. Rev.* **18**, 210 (1921)

2 A. J. Bradley: *Phil. Mag.* **48**, 477 (1924)

3 U. Yoshida: *Jap. Journ. Phys.*, **4**, 133 (1927)

S. Takeyama: *These Mem.*, **12**, 257 (1929)

The Crystal Forms of Metallic Selenium

The general appearance of the crystals deposited on the wall of the inner glass tube was as follows. The largest crystals grew at the part of the highest temperature in every case. This temperature was 210° and about 10° below the melting point of selenium (220.2°). The crystals became smaller in size with decrease of the temperature, and from about 156° the individual crystals became so small that they formed a continuous film with a metallic luster around the glass tube till about 120° . Below this temperature the film lost its metallic luster. This continuous black film gave place gradually between 50° - 60° to a thin red film which is generally known as the red amorphous selenium. The crystals, excepting those in the red film, formed by the condensation of the vapour from molten selenium were thus transformed to the metallic modification.

Table I

Indices	Spacings in Å		Order of Intensity	
	Calc.	Obs.	Obs.	Bradley
0001	4.962	—	—	—
1010	3.776	3.776	2	2
1011	3.008	3.008	1	1
0002	2.481	—	—	—
1120	2.182	2.182	7	6
1012	2.075	2.070	5}	3
1121	1.997	1.998	6}	
2020	1.888	1.888	20	16
2021	1.766	1.763	3	4
0003	1.654}	1.642	9	10
1122	1.638}			
1013	1.516}	1.509	8	10
2022	1.504}			
1230	1.428	1.432	4	5
1231	1.372	1.379	13	12
1123	1.318	1.322	16	15
3030	1.259	1.252	15	19
2023	1.245}	1.237	14	9
0004	1.240}			
1232	1.238}	1.191}	17	15
3031	1.220}			
1014	1.179	1.182}	11	14
3032	1.123	1.124}		
2240	1.091}	1.084	10	7
1233	1.081}			
1124	1.079}	—	—	—
2241	1.065	—	—	—
1340	1.048	—	—	20
2024	1.037}	1.032	12	18
1341	1.025}			
3032	1.003}	1.005	19	17
2242	.999}			
1342	.965}	.968	18	17
1015	.960}			

The crystals formed at the highest temperature were acicular in form, about a centimetre long and 0.1–0.5 mm in diameter, as shown in Fig. 1, Plate I. To examine the lattice form of these crystals, a powder photograph was taken with the powder of them. The results obtained with this photograph are shown in Table I. In the third column of the table are the observed spacings. These spacings when compared with Hull's chart showed close agreement with those of the hexagonal lattice having the axial ratio $c : a = 1.138 : 1$. The calculated values of the spacings given in the second column were obtained by taking 3.776 \AA and 3.008 \AA as the values of the spacings of the $10\bar{1}0$ and $10\bar{1}1$ faces, respectively for reference. These spacings were measured more accurately than others by taking a photograph with a greater distance between the specimen and the photographic plate. As the spacings calculated from both $\text{CuK}\alpha$ and $\text{K}\beta$ reflections for the same plane give the same values for these two planes respectively, these values are used for the calculation of the other spacings given in the second column. In the first column are the indices of various planes of the hexagonal lattice. The fourth and fifth columns give the order of intensity observed by the writer and by Bradley respectively. The numbers in these columns indicate the order of intensity of the spectral lines estimated with the naked eye by taking the most intense line as 1 and the next as 2. From this table the dimensions of the unit cell can be obtained as $a = 4.360 \text{ \AA}$ and $c/a = 1.138$. These values Bradley reported as $a = 4.35 \text{ \AA}$ and $c/a = 1.14$, and K. Slattery¹ as $a = 4.34$ and $c/a = 1.14$ respectively. From the accepted value (4.80) of the density of metallic selenium, the number of the atoms of selenium associated in a unit cell of the crystal is calculated with the X-ray data obtained by the writer to be 2.98.

The Laue-photographs of the continuous films of selenium both with and without the metallic luster mentioned before showed rings having the same spacings as the acicular crystals described above. No indication of fibrous arrangement was observed in these cases. It can be seen from this that these two films are also composed of small crystals of metallic selenium. The rings of the film with metallic luster consisted of many small individual specks, which shows that the crystals of not very small size are arranged in the film with random orientations. The crystal grains in the film without metallic luster were so small that the rings were continuous.

1 K. Slattery: Phys. Rev., 25, 333 (1925)

The greater part of the acicular crystals formed at the part of the highest temperature were hollow prisms and were bounded by several thin walled side surfaces, and some fully developed crystals had six side surfaces, each of which was at an angle of 120° to its neighbours. In some cases these crystals grew in a cluster starting from a common center as is shown in Fig. 2, Plate I. The Laue-photographs of these acicular crystals showed perfect Laue-spots, and the side surfaces of every crystal were seen to be bounded by $(10\bar{1}0)$ planes of the hexagonal lattice with the trigonal axis kept in its lengthwise direction.

When the sections of the walls of these hollow crystals were examined under the microscope in the direction perpendicular to the trigonal axis, there appeared parallel equidistant striations running along the direction of the trigonal axis on the surfaces of the sections, and it seemed that the walls of the crystals consisted of many parallel thin layers parallel to the $(10\bar{1}0)$ planes. The thinnest of these thin layers were estimated to be 0.5μ under the microscope. Some layers had a thickness several times that of the thinnest. Thus, these parallel layers were so thin and were arranged so parallel to each other that no indication of non-parallel growth of the crystal could be observed in the Laue-photograph of the crystal. Such parallel growth of crystals has already been observed in the case of zinc and cadmium crystals¹ formed by the condensation of the vapour, the layers being parallel to the (0001) plane of the hexagonal crystal and the thinnest of these layers being estimated to be 0.8μ for cadmium. Also, Goetz² found that the shortest side of the triangular pattern over an undisturbed area on the main cleavage plane of the bismuth crystal was always the same, and the length of the basal side of this smallest triangle was estimated to be $1.4 \pm 0.2 \mu$. He reported this fact as an experimental verification of the existence of a secondary or mosaic structure³ of the crystal defined by a periodic change in density. As to the numerical value of the period of the secondary structure, Zwicky gave the approximate range from the theoretical standpoint as $0.01 \mu - 1 \mu$, the tendency being for heteropolar crystals to favour the lower end of the scale and for homopolar substances to have large spacings. If the observed facts stated above have some relation to the mosaic

1 M. Straumanis: *Zeits. phys. Chem.*, B, **13**, 316 (1931)

2 A. Goetz: *Proc. Nat. Acad. Sci.*, **16**, 99 (1930)

3 F. Zwicky: *Proc. Nat. Acad. Sci.*, **15**, 816 (1929)

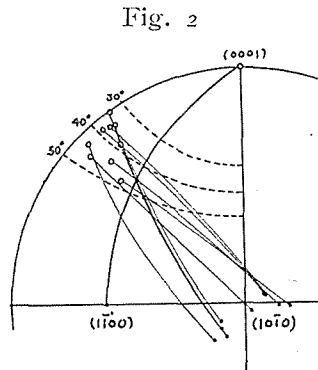
structure of the crystal, the value found by the writer agrees qualitatively with the approximate range given by Zwicky, as metallic selenium may be regarded as partially homopolar.¹

Some of the acicular crystals had side branches with nearly equal inclinations to the stem crystals, as shown in Fig. 4, Plate I, and some smaller crystals formed at the parts of lower temperatures had forms like open or closed V-shaped gauges and the angles between the two component crystals were nearly equal to the angles of the inclinations of the side branches stated above. To see whether or not those crystals form true crystallographic twins of the same type, they were examined by the same method as was used in the case of mechanical twins in tin and zinc.² The results of that examination are given in Fig. 2, in which the mutual orientations

of two component crystals are shown in a part of a stereographic projection on one of the $(10\bar{1}0)$ planes of a component crystal. The orientation of the other component crystal referred to the crystal having one of its $(10\bar{1}0)$ planes as the plane of projection, is indicated by a small circle and a dot connected by an arc which show the direction of the trigonal axis and that of the normal of one of its $(10\bar{1}0)$ planes respectively. As can be seen from this figure, though the mutual orientations of two crystals which form either side branches or V-shaped gauges are somewhat alike, they may not be called true crystallographic twins of the same type. In these cases the trigonal axis of each crystal was always parallel to the lengthwise direction of the crystal.

In some cases when the temperature of the molten selenium was lowered to about 250° , several crystals were obtained whose forms were thin flat plates somewhat elongated in one direction. These crystals also showed perfect Laue-spots, and the flat surface of the plate was parallel to one of the $(10\bar{1}0)$ planes and the lengthwise direction of the elongated plate was parallel to the trigonal axis.

On the other hand, when the temperature of the molten selenium was increased to about 300° there appeared at the part of the highest



1 J. D. Bernal: *Trans. Faraday Soc.*, **25**, 367 (1929)

2 K. Tanaka and K. Kamio: *These Memoirs*, **14**, 79 (1931)

temperature some acicular crystals, each of which was a bundle of many thin needles of perfect crystals and they had a common trigonal axis parallel to the axis of the bundle. The rotation of these needle crystals around the common trigonal axis was seen from their Laue-photographs to be very different according to the case, ranging from a rotation of a few degrees to a nearly perfect fibrous arrangement. When the temperature was raised to more than 300° the forms of the crystals became more and more irregular and no individual crystal was any longer perfectly single, but a fibrous structure of micro-crystals about the trigonal axis or a cluster of such fibers. One of the typical crystals formed at higher temperatures is shown in Fig. 5, Plate I, which is a cluster of two sets of crystal blocks. Any one block of such crystals belonging to either set when separated gave a Laue-photograph of nearly perfect fibrous structure having the trigonal axis as its axis in the lengthwise direction of the block. The Laue-photograph taken normally to the flat crystal at the position indicated in Fig. 5, Plate I, is shown in Fig. 6, Plate I, in which the vertical direction corresponds to the lengthwise direction of the crystal as a whole. This figure when analysed was seen to be due to two sets of incomplete fibrous arrangement whose axes are parallel to the trigonal axes of the crystals and are nearly parallel to the photographic plate. The directions of the two common axes are indicated by the arrows in the figure. The angle between these two axes was about 115° in this case, and for other crystals of the same type it was nearly the same, differing from this value by only one or two degrees. As the directions of these axes are parallel to the directions of the lengthwise directions of the crystal blocks of both sets, the crystal of this type is a cluster of two sets of crystal blocks of incomplete fibrous arrangements of micro-crystals and each block has a parallel common trigonal axis. Another form is shown also in Fig. 7, Plate I, which has a similar arrangement of the micro-crystals to the one shown in Fig. 5, Plate I. The only difference in these two cases is in the angle between the fiber axes of the two sets of the fibrous arrangements. This angle is about 84° in the case of Fig. 7, Plate I.

Crystals with lamellar form such as were reported by Brown were also observed by the writer among the acicular crystals. One of these crystals is shown in Fig. 8, Plate I. This type of crystal gave a Laue-photograph of a fibrous arrangement of the micro-crystals about the trigonal axis, with various rotation of the micro-crystals around

the common axis, which was parallel to the directions of parallel striations appearing on the flat surface of the lamellar crystal.

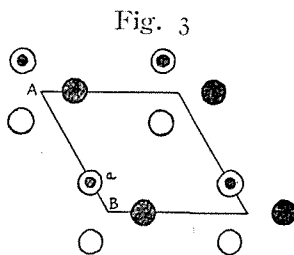
Individual crystals grown at the parts of lower temperatures were clusters of crystals of various degrees of perfection grown parallel to the trigonal axis, and crystals with fibrous structure about the same axis.

No appreciable difference in the formation of the crystals of selenium was observed whether they were formed in a vacuum or in the air at atmospheric pressure.

Growth of the Metallic Selenium Crystals

As can be seen from the forms of crystals of metallic selenium grown by the condensation of the vapour of selenium, the trigonal axis and the $(10\bar{1}0)$ planes of the crystal play important rôles in the process of the growth of the crystal as the most favourable direction of growth and as the boundary surface of every crystal. In the case of the growth of zinc and cadmium crystals¹ formed by the condensation of the vapour, the observed facts were interpreted by the theory of the growth of homopolar crystals developed by Kossel² and Stranski³ and good agreement was obtained between the observed facts and the theory.

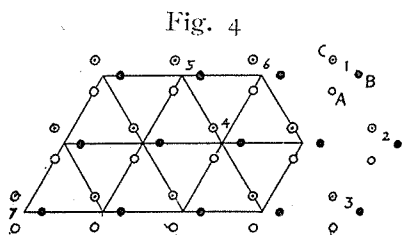
In order to interpret the process of the growth of the crystals in metallic selenium some considerations were made along the same lines as those referred to above. The arrangement of atoms in the crystal lattice of metallic selenium given by Bradley is shown in Fig. 3 as a basal projection of the unit cell of the hexagonal modification of selenium which is composed of three interpenetrating, simple triangular lattices. The spacing (0001) of every simple lattice is equally divided into three parts by the basal planes belonging to other two lattices. In the figure, the differently shaded circles represent atoms at different levels with $c/3$ intervals between them along the trigonal axis. In such a structure the atoms are arranged in three-fold spirals



1. M. Straumanis: loc. cit.
P. A. Anderson: *Phys. Rev.*, **40**, 596 (1932)
2. W. Kossel: "Quantentheorie und Chemie," **1** (1928)
3. I. N. Stranski: *Zeits. f. phys. Chem.*, B, **11**, 342 (1931)
I. N. Stranski and R. Keischew: *Zeits. f. Krist.*, **78**, 373 (1931)

around the trigonal axes allowing two enantiomorphous forms, either right- or left-handed spirals, which are indistinguishable by the method of X-ray analysis. The value of the ratio of the distance aB to that of AB measured on the projection in Fig. 3 was given by Bradley as 0.2166.

According to the theory of crystal growth, it is assumed that in the case of an ideal homopolar crystal, each atom which condenses on a different lattice point on the surface of the crystal is acted on by a force which is qualitatively proportional to the number of contiguous lattice atoms weighted by the distances of them from the atom considered, and the crystal growth takes place by the repetition of this process, by the completion of which maximum energy is liberated. Now we consider the condensation of one atom on various lattice points on the surface of the selenium crystal, assuming for the present that it is a homopolar crystal.



In Fig. 4, atoms in the same lowest level are marked A, those in the middle level B and those in the highest level C respectively. The spirals to which these atoms belong are marked 1, 2, etc. The spirals connected by the straight lines in the figure are those which

are already filled by the lattice atoms, and the spirals 1, 2 and 3 in the same figure represent the positions of the spirals which are to be filled by condensing atoms. Table II shows the numbers of the atoms which are contiguous to each atom in the interior of the lattice. In the table such numbers are arranged in the inverse order of their distances from the atom considered. Of these atoms, those at the distances r_1 , r_3 and r_6 belong to the same spiral as the atom considered

and those at the other distances belong to the neighbouring spirals. Table III is the case of the condensing of one atom on various lattice points on the side surfaces of the hexagonal crystal. In this case

Table II

No. of contiguous atoms	distance	
2	$r_1(2.33 \text{ \AA})$	same spiral
4	$r_2(3.47)$	different ..
2	$r_3(3.69)$	same ..
6	$r_4(4.36)$	different ..
4	$r_5(4.94)$	different ..
2	$r_6(4.96)$	same ..

Table III

Position to be filled	No. of Contiguous Atoms at		
	r_2	r_4	r_6
1 A	3	2	1
1 B	0	2	1
1 C	1	2	2
1	4	6	4
2 A	1	1	1
2 B	0	1	0
2 C	1	1	1
2	2	3	2
2 A (1,3 filled)	3	3	2
2 B (")	0	3	2
2 C (")	3	3	2
2 (")	6	9	6

there is no lattice atom at the distances r_1 , r_3 and r_6 from the point considered. The number of the lattice atoms in the crystal which are contiguous to each lattice point to be filled by one atom by its being condensed on the surface of the crystal, and their distances from the lattice point considered, are given in this table. According to the theory already referred to, these numbers are qualitatively proportional to the forces attracting one atom to the lattice position considered, or the energies to be liberated by the condensing of one atom at that position. Therefore, Table III may be regarded as the table showing the probability of one atom condensing at the position marked or the energies to be liberated by the condensing of one atom at that position. In other words, it may be regarded as a table showing the probabilities of one atom condensing at various lattice positions. The probability for spiral 1 is $4/6/4$, in the usual symbols, and is equal to that for spiral 3 and its equivalent spirals. This value is larger than $2/3/2$ which is the probability for spiral 2. Therefore, the most probable position for the condensation of one atom on the side surfaces of the crystal is in spiral 1, or 3 or its equivalent spirals. Table IV shows how the second atom will be laid after one of the most probable positions, 1A for example, has already been filled by one atom. In this table 1C has two series of numbers of contiguous atoms, the

Table IV

Position	No. of Contiguous Atoms at					
	r_1	r_2	r_3	r_4	r_5	r_6
1 B (1A filled)	1	0	0	2	1	0
1 C (")	1}	1	0}	2	2	0
1 A (Contiguous level)	0}	3	1}	2	1	1
	0		0			
1 (")	2}	4	0}	6	5	1
	1}		1}			
3 A (")	0	1	0	2	2	0
3 B (")	0	0	0	2	1	0
3 C (")	0	3	0	2	1	0
3 (")	0	4	0	6	4	0

upper series is for 1C just below the point 1A and the lower one is for 1C above the point 1A across the point 1B. The probability that the second atom will be added to spiral 1, of which one point 1A has already been filled, is $\frac{2}{1} \cdot \frac{2}{4} \cdot \frac{1}{6} \cdot \frac{1}{5} \cdot \frac{1}{1}$ and is much greater than the probability, $\frac{0}{0} \cdot \frac{1}{4} \cdot \frac{1}{6} \cdot \frac{1}{4} \cdot \frac{1}{0}$, of the addition of the second atom to any other most probable position. This shows that when one atom is already laid on the side surface of the crystal then the second atom has a greater tendency to grow on the spiral which is already occupied by the first atom than to occupy any first position in other new spirals. The crystal thus grows in the side directions by forming new spirals in such positions as 1 or 3 or its equivalent positions. If the crystal grows like this, then it will be bounded by the (11 $\bar{2}$ 0) planes as side surfaces. In Table III, however, when spirals 1 and 3 have been formed the probability that a new spiral will be formed in position 2 is $\frac{6}{9} \cdot \frac{1}{6}$ and is greater than that ($\frac{4}{6} \cdot \frac{1}{4}$) for any other positions, such as 1 or 3. Therefore, the crystal grows in the side directions always forming new spirals so as to be bounded by (10 $\bar{1}$ 0) planes as its side surfaces. This agrees with the observed fact stated before.

Next, we consider the growth along the trigonal axis. Table V

Table V

Position	No. of Contiguous Atoms at	
	r_2	r_3
4 A	2	2
4 B	2	2
4 C	2	2
4	6	6
5 A	2	1
5 B	0	2
5 C	2	1
5	4	4
6 A	2	1
6 B	1	1
6 C	0	1
6	3	3
7 A	0	1
7 B	2	0
7 C	0	1
7	2	2

shows the numbers of lattice atoms contiguous to any point on the (0001) plane of the crystal. In this case, the point where one atom is most likely to be added on the (0001) surface is in a spiral such as 4, which is in the interior of the body of the crystal. The next most probable point is in a spiral such as 5 which is on the surface of the crystal. Spirals at the corner such as 6 and 7 are the least probable sites. This means that the crystal will tend to grow in a prismatic form which becomes thinner as it grows along the trigonal axis, and this also fits the facts.

Table VI

Position	No. of Contiguous Atoms at					
	r_1	r_2	r_3	r_4	r_5	r_6
4	1	6	1	0	6	1
5	1	4	1	0	4	1
6	1	3	1	0	3	1
7	1	2	1	0	2	1
1	0	4	0	6	4	0
2	0	2	0	3	2	0

The great tendency of the metallic selenium crystal to grow along the trigonal axis will be still more clearly seen from table VI. Furthermore, this tendency may be increased when we consider the nature of the bondings between the atoms of metallic

selenium. Among the neighbouring atoms in the lattice, the two atoms at the distance 2.33 Å belonging to the same spiral are in much closer contact than the others, which suggests that there is much greater cohesion between the atoms in the same spiral than between those in neighbouring spirals. Bradley stated in his paper, referred to before, that in the normal crystalline forms of carbon, silicon, germanium, grey tin, arsenic, antimony, bismuth, selenium and tellurium, electron-sharing takes place until the outer shell of each atom has its full quota of electrons and in this way each atom of these elements is in close contact with as many neighbours as it has negative valencies. In this connexion, Bernal¹ considered that homopolar bonds link the atoms in spiral chains, the bond holding the chains together being metallic. Also, it has been pointed out by Hume-Rothery² that the atoms are bound into spiral chains by co-valent bonds so that each chain is in effect an immense molecule, and the different chains are bound together by forces which may be of a molecular nature. Either of these

1, J. D. Bernal: loc. cit.

2. Hume-Rothery: *Phil. Mag.*, **9**, 65 (1930)
The Metallic State (1931)

views implies that there is greater cohesion along the trigonal axis than in other directions, so that the crystals will grow in thin acicular forms, along the trigonal axis, as was observed.

Examination with Convergent X-rays

In order to see the manner of arrangement of the crystal grains in acicular crystals some of them were examined by the convergent X-ray method devised by T. Fujiwara¹. A Shearer metallic tube with copper target was used. The semivertical angle of the primary rays limited by the slit was about 10° and the slit opening was 0.2–0.5 mm. To see the correspondency between the Laue-spots and the spectral lines both reflected by the same atomic planes in the crystal and to obtain the position of the image of direct rays normal to the photographic plate, first the photograph was taken with convergent X-rays with a small lead patch covering the central portion of the photographic plate, then the lead patch was taken off and an ordinary Laue-photograph was taken on the same plate by inserting a second pin-hole slit in front of the first one so that the primary rays limited by these two slits ran in the direction normal to the photographic plate. Thus the spectral lines and the Laue-spots of the same crystal and the image of the direct rays were obtained on a single photographic plate and the comparison between them was made very easily. One of these photographs is shown in Fig. 1, Plate II.

In these photographs taken with convergent X-rays, some crystals showed spectral lines which were composed of several component lines. One of such spectral lines is enlarged and reproduced in Fig. 2, Plate II, which is a $K\alpha$ reflection composed of several component lines reflected by a $(20\bar{2}1)$ plane. In the case of tungsten crystals obtained by deposition, Fujiwara² concluded that some of these component lines are due to several thin sheets of crystal layers which are arranged parallel to each other at small intervals in an individual crystal.

To see whether this is the case or not with the acicular crystals of selenium, the intervals between any two consecutive components of the spectral lines were measured with Hilger's travelling micrometer for several lines. One of the results is given in Table VII. Two

-
1. T. Fujiwara: *These Memoirs*, **11**, 283 (1928)
 2. T. Fujiwara: *These Memoirs*, **13**, 149 (1930)

Table VII (20 $\bar{2}$ 1)

Spectral lines	Distances between two consecutive components		No. of the crystal grains	Angular separation between two consecutive grains
	2.5 cm.	3.5 cm.		
1 $\left. \begin{matrix} a_2 \\ a_1 \end{matrix} \right\}$	} 76	104	1	} 5'10"
2 a_1	} 71	107	2	
3 $\left. \begin{matrix} a_2 \\ a_1 \end{matrix} \right\}$	} 128	{ 86 98	3	} 8'16"
4 $\left. \begin{matrix} a_2 \\ a_1 \end{matrix} \right\}$	} 90	113	4	} 8'47"
5 $\left. \begin{matrix} a_2 \\ a_1 \end{matrix} \right\}$	} 70	109		} 0
6 a_1	} 164	134		
	} 73	100	5	
6 a_1	} 117	142	6	} 3'37"
1 β_1	} 56	81	1	} 3'59"
2 β_1	} 110	160	2	} 8' 5"
3 β_1	} 140	195	3	} 8'54"
4 β_1	} 187	188	4	} 0
5 β_1	} 91	109	5	
6 β_1			6	} 2'53"

photographs at distances of 2.5 and 3.5 cms. were taken with convergent X-rays. In the first column of the table are given the kind of the spectral lines belonging to the crystal grains marked by the number. The second and the third columns are the distances measured in μ between two consecutive lines on the photographs taken at the distances of 2.5 and 3.5 cms. respectively. The calculated distances between the components of the α doublet are 73.3μ and 102.5μ respectively. From this table it is seen that the separation between two corresponding spectral lines due to two consecutive crystal grains measured at two different distances is not always the same and the values for 3.5 cms. are larger than those for 2.5 cms. except for grains 4 and 5. This indicates that only two grains, 4 and 5, are arranged parallel to each other in this case, and the other grains are inclined at small angles to each other. The angle between two consecutive grains is calculated from the separations between the two corresponding spectral lines at different distances, and these are shown in the fourth column of the table. The corresponding angles obtained from the α and β lines are nearly equal.

One of the crystals examined showed the spectral lines shown in Fig. 3, Plate II, which consisted of two sets of bands containing some

lines. The radial breadths of these bands in the photographs taken at different distances give an approximate measure of the angular distribution of the micro-crystals around a common axis. Thus it was found that the angular distribution of the orientation of the micro-crystals in the two imperfect grains were $49'$ and $51'$ respectively around the trigonal axis of the crystal. The micro-crystals contained in two imperfect grains were so large that they gave rise to rather separate spectral lines in the bands. The Laue-photograph of this crystal was seen to consist of two sets of imperfect Laue-spots of nearly equal orientation. This is in accordance with what was stated above.

Crystals with fibrous structure of the micro-crystals such as lamellar forms gave photographs such as that shown in Fig. 5, Plate II. Fig. 4, Plate II is a photograph taken by means of the convergent X-rays, with an acicular crystal compressed mechanically in the direction normal to the trigonal axis of the crystal, and is due to a fibrous arrangement of the micro-crystals around the trigonal axis. The difference between the two photographs mentioned above is that the micro-crystals produced by the destruction of the acicular crystal by compression are so small in size that they give only continuous bands limited by the divergency of the incident X-rays; while in the case of Fig. 5, Plate II, the crystal grains composing the fibre are large in size and few in number and they are arranged discontinuously around the common axis.

If the size of a perfect single crystal is smaller than the opening of the slit so that the whole crystal is exposed to the primary beams, the size will be given approximately from the radial breadth of each spectral line. In such a case the radial breadth of the same spectral line measured at different distances from the crystal will be equal. On the contrary, when the crystal is imperfect and the orientation of the micro-crystals composing the crystal is somewhat scattered, the radial breadth of the spectral line at different distances may vary. Thus the size and the degree of perfection of the crystal can be estimated from the radial breadths of the spectral lines measured at different distances.

Table VIII gives the values, measured in μ , of the radial breadths of four spectral lines photographed at the distances of 1.5, 2.5 and 3.5 cms. with the same crystal. The components of the α doublet

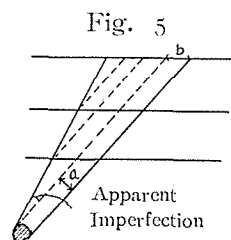


Table VIII

	10 $\bar{1}$ 0 β_1		10 $\bar{1}$ 0 $\alpha_{1,2}$		11 $\bar{2}$ 0 β_1		11 $\bar{2}$ 0 $\alpha_{1,2}$	
	Breadth in μ	Diff.	Breadth in μ	Diff.	Breadth in μ	Diff.	Breadth in μ	Diff.
1.5 cm	80	15	103	27	91	19	107	33
2.5 cm	95		130		110		140	
3.5 cm	109	14	154	24	130	20	174	34
b	62		65		61		56	
a	57		59		49		44	
Apparent Imperfection			7' 5"				7' 3"	
Doublet Separation			1' 49"				3' 17"	
Imperfection	4' 12"		5' 11"		4' 22"		3' 46"	

were not so sharply separated on the photographic plate that they could be measured separately in this case, and the breadth were measured by regarding this doublet as a single spectral line. The differences of the breadths of the corresponding spectral lines on two photographs taken at two consecutive distances should be the same in this case, as was actually observed. From these differences the breadths b and a shown in Fig. 5 were calculated. The breadth a may be looked upon as the size of the crystal exposed to the X-rays. The maximum breadth of the crystal examined was also measured with a microscope in the direction parallel to the photographic plate, and it was found to be 65, roughly in accordance with the values of a given in the table. The angle of rotation of the micro-crystals around an axis normal to the plane of the figure in Fig. 5, which is called an apparent imperfection in the same figure, is given also in the table. In the case of the α doublet which is not sharply separated on the photographic plate, the angle given as apparent imperfection in the table is composed of two parts. The one is the angle due to the doublet separation and the other is the angle of rotation of the micro-crystals. As is seen in the table, the values of a and the imperfection measured with the α and β lines caused by the same atomic plane are nearly equal respectively. This fact seems to be easily understood from the smallness of the angle between the α and β lines reflected by the same atomic plane. The crystal examined above was the most perfect one treated by the writer, yet it was not entirely perfect and

disclosed some defect, as is shown in the table. The presence of such a defect in the crystal seems to be an important factor in preventing the growth of the crystal to a much larger size.

Some spectral lines obtained with convergent X-rays show non-uniform intensity distributions along the lines themselves. This effect was considered by T. Fujiwara¹ to be due to the intensity distribution of the characteristic radiations at various starting points on the surface of the target. To examine this effect more closely, some photographs were taken with a copper target with sixteen parallel scratches of 0.5 mm depth at an interval of $\frac{3}{4}$ mm on its surface. The intensity distribution of the primary X-rays starting from the surface of this target can be seen in the pin-hole photograph shown in Fig. 6, Plate II, which differs greatly from the photographs taken with the usual target with plane surface, such as Fig. 7 or Fig. 8, Plate II. To see whether the intense parts correspond to the scratches on the surface of the target or not, one more scratch of the same depth was made on the same surface crossing the original scratches. The pin-hole photograph showed a weaker line corresponding to the new scratch. Therefore, when there are some irregularities on the surface of the target more intense radiations may be expected to start from the parts of higher elevation on the surface of the target. Several photographs were taken with convergent X-rays starting from such a target. One of them is shown in Fig. 1, Plate III. From the fact that the inclination between the spectral line and the parallel striations of different intensities is nearly equal to that expected from the inclination between the direction of the parallel scratches and the line of intersection of the surface of the target with the reflecting cone of the atomic plane of the crystal for the incident beam, it can be seen that such intensity distributions in the spectral lines themselves, as stated above, are due to the intensity distribution of the characteristic radiations at the starting points on the surface of the target. This point was also confirmed by taking another Laue-photograph (Fig. 2, Plate III) of the same crystal with the usual target without any scratches on its surface. The clear striations in the spectral lines seen in Fig. 1, Plate III, disappeared in this case.

The intensity distribution of the primary X-rays at the starting points on the surface of the target are also affected by the shape of the aluminium cathode. Figs. 7 and 8, Plate II are two pin-hole

1. T. Fujiwara: *These Memoirs*, **13**, 303 (1930)

photographs taken with the same target and with different cathodes. In the case of Fig. 8, Plate II, a newly polished cathode was used, and in the other case a cathode whose shape had become modified by being used for a long time, was employed. This difference in the distribution of the intensity of the X-rays thus resulting at the surface of the target gives rise immediately to a change in the intensity distribution along the spectral line.

Vitreous and Amorphous Selenium

When metallic selenium is heated above its melting point, 220°C , it melts and turns to a liquid which on rapid cooling does not return to its original metallic form but becomes more and more viscous till about 60° as a super cooled liquid. Below this temperature and at room temperatures it is a hard and brittle mass and is known as vitreous selenium. The X-ray photograph of the powder of the vitreous selenium, taken with the copper $K\alpha$ radiations, is shown in Fig. 3, Plate III, which shows only a single broad diffraction band similar to those obtained with liquids or glasses. Amorphous selenium is a fine red powder. This form is obtained in several ways, such as by the reduction of selenious acid or by the addition of water to the solution of selenium in concentrated sulphuric acid or by the condensation of the vapour from molten selenium. The writer examined the amorphous selenium obtained by the second method with X-rays, and it was observed that it gave the same diffraction band as the vitreous one. As the other properties are also the same, these two forms are regarded as the same substance differing only in the state of aggregation.

When the vitreous selenium is warmed, it begins to soften at about 50° – 60° and becomes viscous, and on continuous heating it becomes hard again. This property is the same for amorphous red selenium. The hard substances thus obtained from both vitreous and amorphous selenium showed the same diffraction rings as the metallic selenium. From this it can be seen that both vitreous and amorphous selenium can be transformed into the metallic form by annealing them at suitable temperatures.

To determine the temperature of this transformation, vitreous selenium was annealed at various temperatures for two hours in every case. Then the specimens were examined with the copper $K\alpha$ radiations, and the transition temperature was seen to lie between 70° and 80° . Three of such photographs are shown in Figs. 4, 5 and 6, Plate

III, which correspond to the annealing temperatures of 73.5° , 74.5° and 76° respectively. The photograph shown in Fig. 7, Plate III was taken similarly with the powder of metallic selenium, and is reproduced for the sake of comparison. The specimens annealed below 73.5° showed a single diffuse band, like vitreous or amorphous selenium. The specimens annealed at 74° and 74.5° showed the diffuse band of vitreous selenium and several weak lines corresponding to the atomic spacings of metallic selenium. This shows that these specimens are mixtures of vitreous and metallic forms. With the specimens annealed at higher temperatures the diffraction lines proper to the metallic selenium became very prominent, and the diffuse band of vitreous selenium became so weak as to be scarcely perceptible. Therefore, it can be seen from the X-ray method that the transition takes place roughly at about 74° .

On the other hand the net densities of the fine powder of the specimens annealed at various temperatures were measured by the method devised by U. Yoshida and B. Takei¹, which is especially suitable for obtaining net densities with porous and powdery substances. The result is shown in Table IX and Fig. 6. The densities of pure vitreous and pure metallic selenium were found to be 4.277 and 4.819

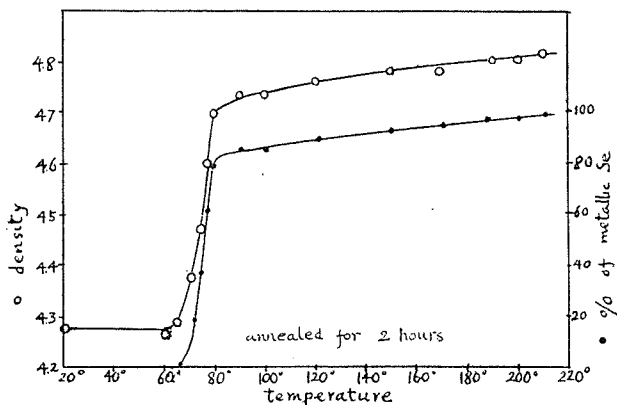
respectively. The value 4.819 was the density of a specimen which was annealed for five hours at 200° after the specimen had been melted in vacuo. From the values of the net densities of the specimens obtained by annealing at various temperatures we can easily obtain the proportion of the mixture of amorphous and metallic selenium. The weight percentages of the content of metallic selenium in the mixtures are shown in Table IX and Fig. 6. This result agrees well with the one obtained by the X-ray examination, and the transition is con-

Table IX (annealed for two hours)

Temperature of Annealing	Density	% of metallic Se
room	4.277	0
60	4.260	0
65	4.287	2
71	4.375	20
75	4.471	38
77.5	4.600	62
80	4.697	80
90	4.732	85
100	4.733	85
120	4.758	90
150	4.777	93
170	4.787	94.5
190	4.800	97
200	4.806	97.2
210	4.816	99

1 U. Yoshida and B. Takei: These Memoirs, 15, 1 (1932)

Fig. 6



firmed to take place at between 67° and 80° .

The red film deposited at the cooler portions of the tube used in Fig. 1. showed also the same broad diffraction band as red amorphous selenium.

Randall, Rooksby and Cooper¹ have supposed from the X-ray examination of several glasses that they consisted of very small crystals (10^{-6} – 10^{-7} cms). Similar considerations may also be applied to our case; and if we consider that the difference between vitreous and metallic selenium is only in the size of the crystal grain but not in the crystal lattice itself, then the net densities of these two substances should be the same. But the above results obtained with the densities refutes this consideration decisively, and we can say that the selenium in the vitreous or amorphous state has not the same crystal lattice as the metallic form and the mean distance between the atoms is greater than in the metallic form.

The softening of the vitreous selenium by heating at temperatures below the transition temperature is explained as its molten state. On further heating up to the transition temperature, the atoms in the liquid state arrange themselves into the crystal lattice of metallic selenium, which causes the solidification of selenium again by heating.

In conclusion, the writer wishes to express his sincere thanks to Prof. U. Yoshida for his kind guidance and invaluable suggestions.

1. J. T. Randall, H. P. Rooksby and B. S. Cooper:
Nature, **125**, 458 (1930)
Zeits. f. Krist., **75**, 196 (1930)

Plate I

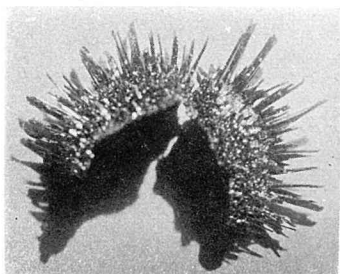


Fig. 1

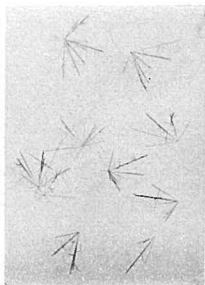


Fig. 2

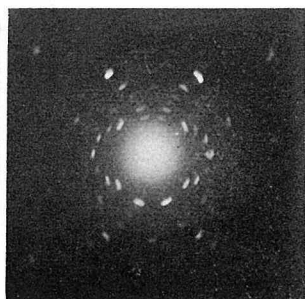


Fig. 3

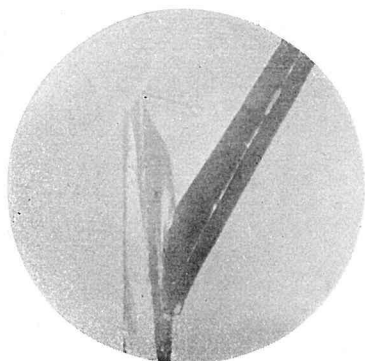


Fig. 4
× 10

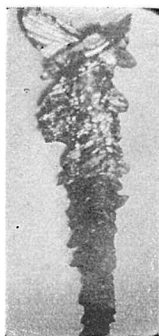


Fig. 5
× 10

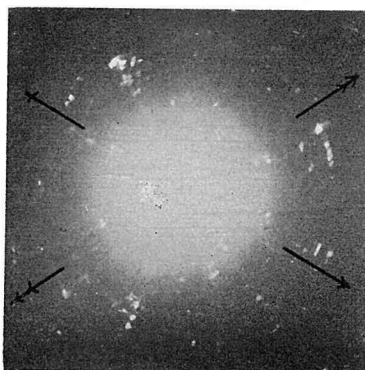


Fig. 6

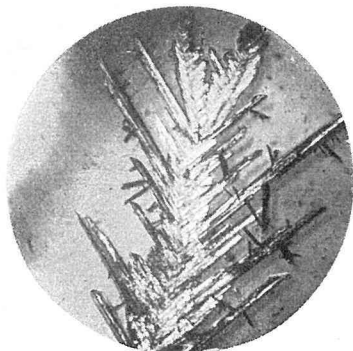


Fig. 7
× 15

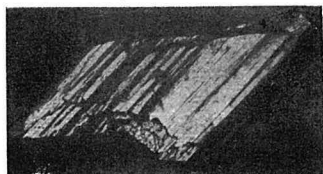


Fig. 8
× 15

Plate II

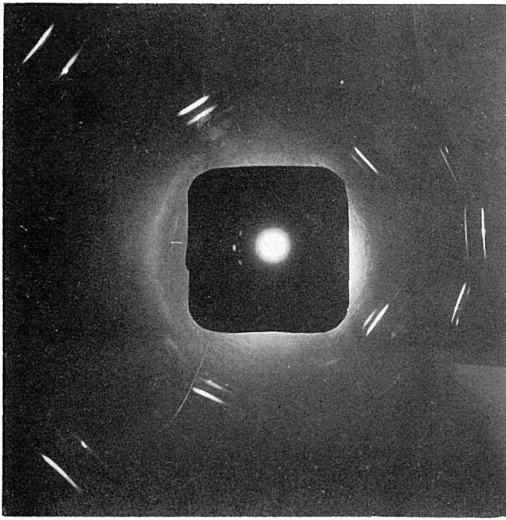


Fig. 1

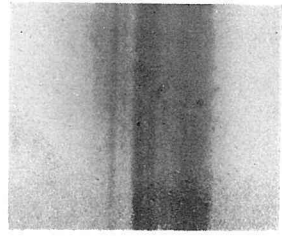


Fig. 2 $\times 15$

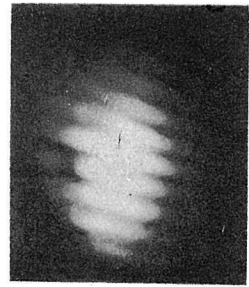


Fig. 6

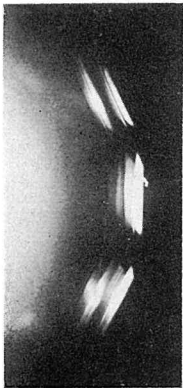


Fig. 3

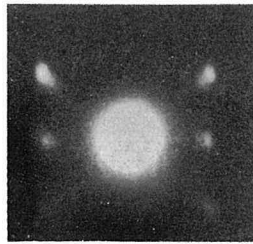


Fig. 4



Fig. 7

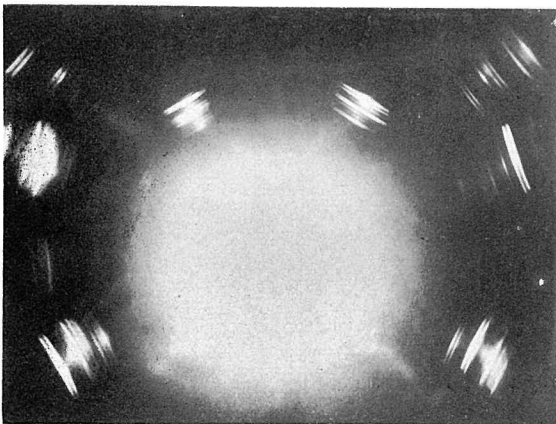


Fig. 5



Fig. 8

Plate III

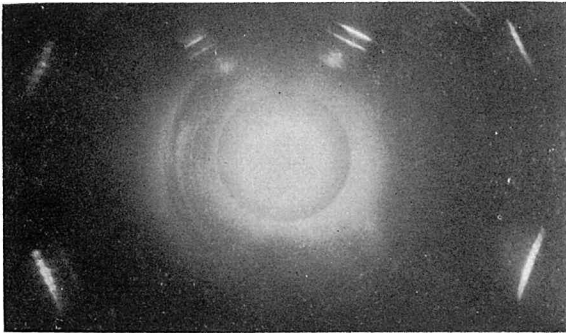


Fig. 1

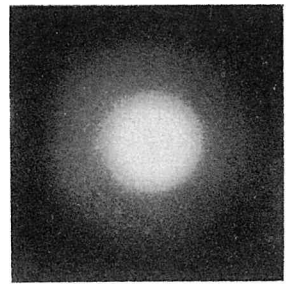


Fig. 3

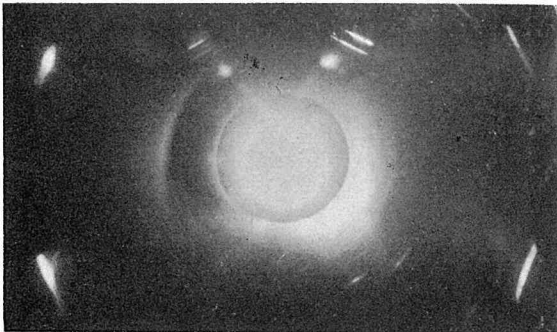


Fig. 2

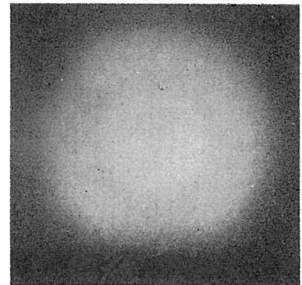


Fig. 4

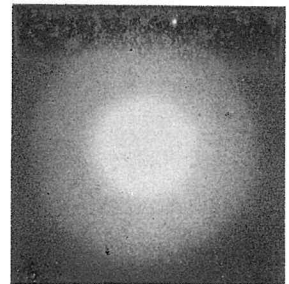


Fig. 5

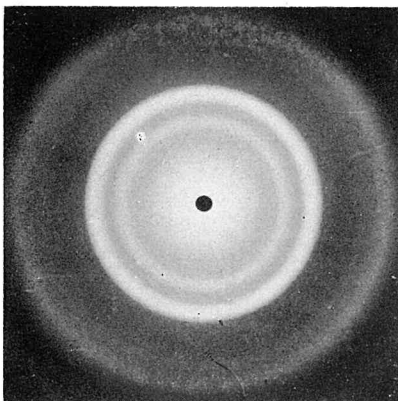


Fig. 7

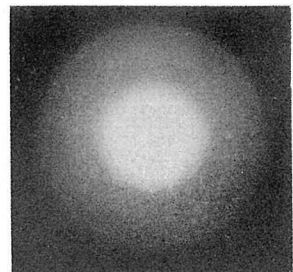


Fig. 6